Journal of Neuroscience Methods 348 (2021) 108985

Contents lists available at ScienceDirect

Journal of Neuroscience Methods

journal homepage: www.elsevier.com/locate/jneumeth

Reproducibility of power spectrum, functional connectivity and network construction in resting-state EEG

Wei Duan [a,b], Xinyuan Chen [a,b], Ya-Jie Wang [a,b], Wenrui Zhao [a,b], Hong Yuan [a,b,c], Xu Lei [a,b,c,*]

[a] Sleep and NeuroImaging Center, Faculty of Psychology, Southwest University, Chongqing, 400715, China
[b] Key Laboratory of Cognition and Personality (Southwest University), Ministry of Education, Chongqing, 400715, China
[c] National Demonstration Center for Experimental Psychology Education (Southwest University), Chongqing, 400715, China

ARTICLE INFO

Keywords:
Resting-state EEG
Power spectrum
Connectivity measure
Network construction
eLORETA
Reproducibility

ABSTRACT

Background: Characteristics from resting-state electroencephalography (rsEEG) provides relevant information about individual differences in cognitive tasks and personality traits. Due to its increasing application, it is crucial to know the reproducibility of several analysis measures of rsEEG.
New method: A new brain network construction method was proposed based on simplified forward model (SFM). In addition, we aimed to carry out an extensive examination of the reproducibility of the power spectrum and functional connectivity at both the sensor-level and the source-level. We systematically proposed multiple new pipelines by integration source imaging, time-course extraction and network reconstruction.
Results/comparison with existing method(s): Our results revealed that the reproducibility of eyes-closed was slightly higher than that of eyes-open, and the relative power was more repeatable than the absolute power, especially in high-frequency bands. The reproducibility of the sensor-level was higher than that of the source-level, both for power and connectivity. Remarkably, connectivity measures could be separated into two classes according to their reproducibility. Notably, the reproducibility of power envelope correlation (PEC) was generally the highest among those connectivity measures which are insensitive to volume conduction effect. For the whole-brain network construction, single dipole modeling was better than the dimensionality reduction methods, such as mean or principal component analysis (PCA) of multiple dipoles of a region.
Conclusions: In conclusion, our results described the reproducibility of rsEEG power spectrum, connectivity measures, and network constructions, which could be considered in assessing inter-individual differences in brain-behavior relationships, as well as automatic biometric applications.

1. Introduction

Resting-state is the state in which a participant is awake and not required to engage in a specific task. This paradigm could reflect the intrinsic activity of the brain (Deco et al., 2011; Greicius et al., 2003). Moreover, for those participants who are difficult to instruct such as children or the aged, the resting-state is more straightforward than the task condition in terms of participant instructions. Compared with breakthroughs in resting-state functional magnetic resonance imaging (rsfMRI) research, there is still a lot of work to be done in resting-state electroencephalography (rsEEG), though its property has been revealed in the first EEG recordings performed in 1929. A favorable feature of fMRI is high spatial resolution. However, this technique has a limited temporal resolution. A considerable part of the fluctuations of brain activity occurred at a time-scale of subsecond (Koenig et al., 2005), and this time-scale was available for EEG. Furthermore, EEG devices have significant advantages in portability and price, which also increases the feasibility of EEG research.

In recent years, there has been a large amount of literature on rsEEG which provided valuable information on the diseased brain, such as in epilepsy (Rotondi et al., 2016), schizophrenia (Siebenhuhner et al., 2013) and Alzheimer's disease (Babiloni et al., 2013). Meanwhile, rsEEG in healthy brains also had many topics as gender differences (Volf et al., 2014) and aging (Tomescu et al., 2018). The wide range of applications has led to an important issue: How reproducible the measures (such as power and connectivity) are at rsEEG? If those measures vary significantly between sessions, this will reduce the statistical power of the experiment to detect a true treatment effect (Deuker et al., 2009).

* Corresponding author at: Sleep and NeuroImaging Center, Faculty of Psychology, Southwest University, Chongqing, 400715, China.
E-mail address: xlei@swu.edu.cn (X. Lei).

https://doi.org/10.1016/j.jneumeth.2020.108985
Received 30 June 2020; Received in revised form 14 September 2020; Accepted 20 October 2020
Available online 24 October 2020

Power spectrum analysis of rsEEG has a long history in EEG analysis, and it can provide the power of a specific frequency. The spectral patterns have been reported to be stable at 12–40 months retest (Napflin et al., 2007), and the amplitude measures had high test-retest correlations (r = .92 at 5 min, .84 at 12–14 weeks, (Salinsky et al., 1991)). Salinsky and colleagues also found there was essentially no difference between the reproducibility of absolute and relative power, and duration with 60 s was nearly as reproducible as those of 40 or 20 s (Salinsky et al., 1991). Alpha and theta bands attracted special attention due to their dominant distributions. Previous investigations revealed that alpha and theta power at frontal and posterior electrodes had higher reproducibility in both healthy adults (Smit et al., 2005) and depressed patients (Bruder et al., 2008). Although previous studies have discussed the reproducibility of power spectral, there are still several issues to consider. First, both eyes-open (EO) and eyes-closed (EC) are natural states for rsEEG. However, these two conditions were associated with specific eye movements (van Diessen et al., 2015), and brain networks (Agcaoglu et al., 2019). Corsi-Cabrera et al. (2007) found that EC was more stable over sessions than EO, but a magnetoencephalography (MEG) study found slightly high reproducibility in the EO condition (Martín-Buro et al., 2016). Second, to minimize the influences of artifacts on the results, different data pre-processing steps were applied. In addition to visual inspection done by the well-trained researchers, several automatic methods were available for artifacts movement (Muthukumaraswamy, 2013; Pion-Tonachini et al., 2019), though it was unknown that to what extent those pre-processing steps influenced the reproducibility of power spectrum. Third, a previous study had found the small effect of short duration (20−60 s, Salinsky et al., 1991). A further examination is certainly needed in a broader time range (0−5 min).

To choose the best method from dozens of connectivity measures in rsEEG, reproducibility should be considered as one of the most critical factors. In a MEG study, Colclough and colleagues found that phase- and coherence-based connectivity measures, such as the phase lag index (PLI) and the imaginary coherency (IMC), had poor reproducibility. Remarkably, the amplitude envelope correlation (AEC) had the best performance (Colclough et al., 2016). However, there were rare investigations focused on the reproducibility of different connectivity measures in EEG. Moezzi and colleagues investigated the reproducibility of IMC and graph metrics in different frequency bands (Moezzi et al., 2018). Moreover, they found the IMC had intra-class correlation coefficients (ICC) values ranging from 0.30 to 0.49 in sensor-level, and smaller in source-level. Compared with MEG, EEG signal was more sensitive to volume conduction effect and had erroneous high connectivity in the scalp surface (Nunez et al., 1997; Schoffelen and Gross, 2009). Therefore, those connectivity measures that are sensitive to volume conduction effects seem to be more unsuitable for EEG. As there is no previous study on the reproducibility of those measures in EEG, both sensitive and insensitive to volume conduction effects measures would be included in this study.

For the whole-brain network construction in rsEEG, the important selections include parcellation of the whole brain and estimating the time series of a region. Usually, a priori anatomical template was utilized as the basis for regional parcellation, for example, the template of Automated Anatomical Labeling (AAL) atlas (Rolls et al., 2020). In fMRI, the averaged time series was extracted for each AAL region, and pair-wise correlations between regional time series were computed to obtain a functional connectivity matrix. In contrast, previous EEG studies have proposed various methods to obtain the time series of each brain region. Some researchers got the activity of each region of interest (ROI) from the first principal component of the dipoles inside a region (Colclough et al., 2016; Iandolo et al., 2020). Meanwhile, the center dipole was used to represent the activity of the whole ROI (Moezzi et al., 2018). Moreover, an alternative strategy could reduce the number of dipoles with the forward model. That means, rather than considering thousands of dipoles, we may simply have about one hundred of dipoles, and each represented an AAL region. Interestingly, there was rare study, to our knowledge, investigating the stability of those methods. In this study, we used a more comprehensive perspective to discuss the reproducibility of resting-state EEG. We recorded rsEEG signals in 57 healthy young volunteers in three 10-minute resting-state sessions separated by one month. We compared several issues of rsEEG, including two resting conditions (EC and EO), four pre-processing steps, seven data durations (4–256 s), two power types (relative and absolute), eight connectivity measures, and four network construction methods. Based on previous studies, we had two hypotheses: (1) The reproducibility of the source-level metrics was smaller than that of the sensor-level ones; (2) The alpha band had the highest stability than any other frequency bands. For other parameters (resting conditions, pre-processing steps, connectivity measures, and network constructions), we did not have any hypotheses. Our exploratory study may reveal the most important parameters to increase the reproducibility of rsEEG.

2. Methods

2.1. Participants and experimental design

A total of 57 healthy participants (24 males, 57 right-handed, 19.7 ± 1.3 *(M ± SD)* years old) were recruited through online advertisement. No history of psychiatric or neurological illness was reported. During resting-state EEG recording, participants were instructed to view a fixation point for 5 min (EO) and then close eyes for another 5 min (EC). They needed to keep still, quiet, and relaxed as much as they can, and try to avoid blinking. We collected EEG signals for three sessions in total, including the present (session 1), 90 min later (session 2), and one month later (session 3). There were 342 recordings (3 sessions × 2 conditions × 57 participants) of 5-minute EEG in our study. No alcoholic, caffeinated food or drink was allowed on the EEG recording date. This study was approved by the Review Board of the Institute of Southwest University. Written informed consent was obtained after a detailed explanation of the study protocol. All experiments were in accordance with the Declaration of Helsinki.

2.2. EEG acquisition and pre-processing

Continuous scalp EEG was recorded by 63 Ag/AgCl active electrodes mounted within an elastic cap, based on the extended 10–20 international electrode placement system (Brain Products GmbH, Steingrabenstr, Germany). Two of these channels were used to record electrooculograms and the FCz was utilized as the online reference channel. The sampling rate was 500 Hz and the electrode impedance was kept below 5 kΩ after careful preparation. EEG data were exported to EEGLAB (version 2019_1, http://sccn.ucsd.edu/) for pre-processing.

We separated pre-processing into 4 steps, and each constructed a gradually improved preprocess strategy, which was an important factor for our reproducibility analysis. We finally got 4 datasets, meaning 4 levels of pre-processing. In the first dataset (Re-reference), the raw data were re-referenced to a common average reference and filtered using a Finite Impulse Response (FIR) filter (0.3–45 Hz). The second dataset (Reject Channel): the raw data were filtered (0.3–45 Hz) and the bad channels were interpolated by surrounding channels. After that, data were re-referenced to a common average reference. On average, 1.94 electrodes were labeled as bad channels (1.94 ± 1.90). The third dataset (Reject Epoch): based on the second data set, the data signal was segmented into epochs of 4 s and bad epochs were rejected. On average, 8.24 epochs of each 5 min recording were labeled as artifact epochs (8.24 ± 4.71). The fourth dataset (Reject ICs): based on the third data set, after running independent component analysis with EEGLAB, some independent components (ICs) were marked as artifacts. On average, 3.01 ICs in each recording were rejected (3.01 ± 2.25).

2.3. Power spectrum analysis

Based on the artifact-free dataset (Reject ICs), we calculated the cross-spectral density matrices using Welch's method (window and segment length: 4S, non-overlap, frequency range: 1:1:45 Hz) and then we got the power spectrum of each channel. The absolute power of each channel was averaged to obtain seven frequency bands, Delta (1−4 Hz), Theta (4−8 Hz), Alpha1 (8−11 Hz), Alpha2 (11−13 Hz), Beta1 (13−20 Hz), Beta2 (20−30 Hz) and Gamma (30−45 Hz). Relative power was obtained by normalizing power in each frequency band with the overall power in 1−45 Hz within each channel in sensor-level or each dipole in source-level.

To investigate the effects of pre-processing, resting conditions and power types on the reproducibility of the power spectrum, we compared 16 combinations of these factors: 2 resting conditions (EC / EO) × 2 power types (Absolute / Relative Power) × 4 pre-processing steps (Re-reference / Reject Channel/ Reject Epoch/Reject ICs). Besides, we also considered the effects of duration, i.e., the signals were restricted to the first 4, 8, 16, 32, 64, 128, and 256 s of all the artifact-free signals after all the pre-processing steps. Notice that 23 recordings did not remain 256 s signal after pre-processing, so their total signals (range from 232 to 252 s) were utilized in these conditions.

2.4. Connectivity measures

Previous EEG studies had employed many connectivity measures. According to coupling modes between neuronal oscillations: phase-coupling and amplitude-coupling, those connectivity measures could be divided into two primary classes: phase-based and amplitude-based (Siems and Siegel, 2020). Here, we only considered some of functional connectivity measures due to their wide application.

First, phase-based measures, including phase lag index (PLI), weighted phase lag index (wPLI), ρ index (RHO) and phase-locking value (PLV) estimated the phase synchrony between two signals according to their instantaneous phase in a particular frequency band (Lachaux et al., 1999; Stam et al., 2007; Tass et al., 1998; Vinck et al., 2011). Besides, coherence-based measures, including coherence (COH), imaginary coherence (IMC) and lagged coherence (LGC) also describe the relation between phases, they should be classified as phase-based measures too. The coherence of two signals is their normalized cross-spectral density. The imaginary coherence (Nolte et al., 2004) is the imaginary part of coherence which is insensitive to the effects of volume conduction. The lagged coherence can be regarded as an improved version of IMC (Pascual-Marqui et al., 2011). Compared to IMC, it is resistant to non-physiological artifacts and is minimally aff ; ected by low spatial resolution.

Second, the amplitude-based method, i.e., power envelope correlation (PEC) calculated the power correlation after removing the zero-lag contribution on all pairs of nodes. One previous study found its superiority in the reconstruction of the resting-state brain networks (Hipp et al., 2012).

In our study, PLI, PLV, RHO, COH, IMC, and LGC were calculated based on the HERMES toolbox (version: 14-04-2015, http://hermes.ctb.upm.es). WPLI and PEC were calculated based on Fieldtrip toolbox (version: 2016_11_08, http://www.fieldtriptoolbox.org). We defined a connectivity measure as insensitive to volume conduction measure if it is insensitive to the linear mixtures of independent signals. For the above eight connectivity measures, IMC, LGC, WPLI, PLI, and PEC are insensitive to volume conduction, besides, PLV, COH and RHO are sensitive to volume conduction.

2.5. Source reconstruction

In our current study, source reconstruction calculations were performed on Fieldtrip software. We used the Colin27 head template anatomies (a detailed MR image made of 27 scans of a single individual head, see (Holmes et al., 1998)). The solution space was restricted to the cortical interface of grey-white matter, corresponding to 8196 dipoles with perpendicular direction to the surface of the cortex. We used the boundary element method (BEM, (Mosher et al., 1999)) as the electrical model. The strength and distribution of cortex sources were estimated with exact low resolution electromagnetic tomography (eLORETA, (Pascual-Marqui et al., 2011)) and the regularization parameter α is 0.05.

Both power and connectivity were estimated at the source-level. The power spectrum of each dipole was calculated by projecting the sensor-level cross-spectral density matrices (63 × 63) into the source space (8196 × 8196) frequency-bin-by-frequency-bin. For connectivity analysis, to increase the comparability of different connectivity measures, we estimated the connectivity matrices using the time series (Colclough et al., 2016; Mahjoory et al., 2017) in the source space.

2.6. Whole-brain network construction

The template of automated anatomical labeling atlas (AAL3, (Rolls et al., 2020)) was used to whole-brain network construction. The 8196 dipoles were segmented into different ROIs by their MNI coordinates. If a dipole lies within an ROI, it will be labeled as that ROI. If a dipole does not lie within any ROI, it will be labeled to the nearest ROI. In this way, there were 101 ROIs that remained in our following analysis.

Four methods were considered to estimate the time series of a region:

(a) The first principal component within each ROI (PCA): the time series of all the dipoles in each region were concatenated, generating a matrix dimension of t × d. Here, t and d represented the number of time points and number of dipoles respectively. Then this matrix was decomposed using principal component analysis. Finally, the first principal component was utilized as the time series of the ROI.
(b) The average within each ROI (AVE): the time series of all the dipoles in each ROI region was averaged to represent the time series of this ROI. The advantage of this method is simple and straightforward, and a similar method was utilized in fMRI.
(c) The center dipole representative (CDR): the time series of the spatial center dipole of each ROI was chosen as the time series of this ROI. This dipole has the smallest Euclidean distance from all the other dipoles of the region (Moezzi et al., 2018). We assumed that the spatial center dipole may be a good representative of an ROI. However, the disadvantage of this assumption is its small signal-to-noise ratio, as a single dipole is very sensitive to noise.
(d) The simplified forward model (SFM): we reconstructed a new forward model with only 88 center dipoles. The location and direction of center dipole were defined the same as in CDR. Then, the time series of each dipole was calculated using eLORETA. This means that our forward model only involves 88 dipoles, rather than original 8196 dipoles. This method has the advantage of lower computation complexity; however, the geometric properties of each ROI were greatly simplified in this model.

2.7. Statistical analysis

We used intra-class correlation coefficients (ICC) to assess reproducibility which is the within-subject between-time reliability. For power spectrum analysis, we calculated ICC on each frequency band at each electrode/dipole. For each connectivity measure, we calculated ICC on each frequency band at each edge.

In the current situation, Y_{ij} denotes the power or the connectivity from the i-th participant's j-th measuring occasions ($i = 1,2, \ldots 57$; $j = 1,2,3$).

$$MS_p = \frac{\mathrm{d}}{\mathrm{n}-1}\sum_{i=1}^{n}\left(\overline{\mathrm{Y}}_i - \overline{Y}\right)^2$$

$$MS_e = \frac{1}{(n-1)\times(d-1)}\sum_{i=1}^{n}\sum_{j=1}^{d}\left(Y_{ij} - \overline{Y_i} - \overline{Y_j} + \overline{Y}\right)^2$$

d(= 3) is the number of sessions and n(= 57) is the number of participants. MS_p is the between-participants mean square and MS_e is the error mean square.

The specific ICC form used here is (Shrout and Fleiss, 1979):

$$ICC = \frac{MS_p - MS_e}{MS_p + (d-1)MS_e}$$

To investigate the relationship between different connectivity measures, the Spearman correlation was utilized between the ICC values of eight connectivity measures. We also conducted repeated measurement ANOVA in each condition, to reveal the mean effect of resting conditions, pre-processing steps, data durations, power types, connectivity measures, and network constructions. In those conditions, the 7 frequency bands were utilized as repeated measurements. The Greenhouse–Geisser correction was used to adjust the effects for any violation of sphericity.

3. Results

3.1. Sensor-level power spectrum analysis

Among all frequency bands, for relative power, beta1 (13–20 Hz) had the highest reproducibility with full pre-processing steps, no matter in EC or EO; for absolute power, theta (4–8 Hz) and alpha1 (8–11 Hz)

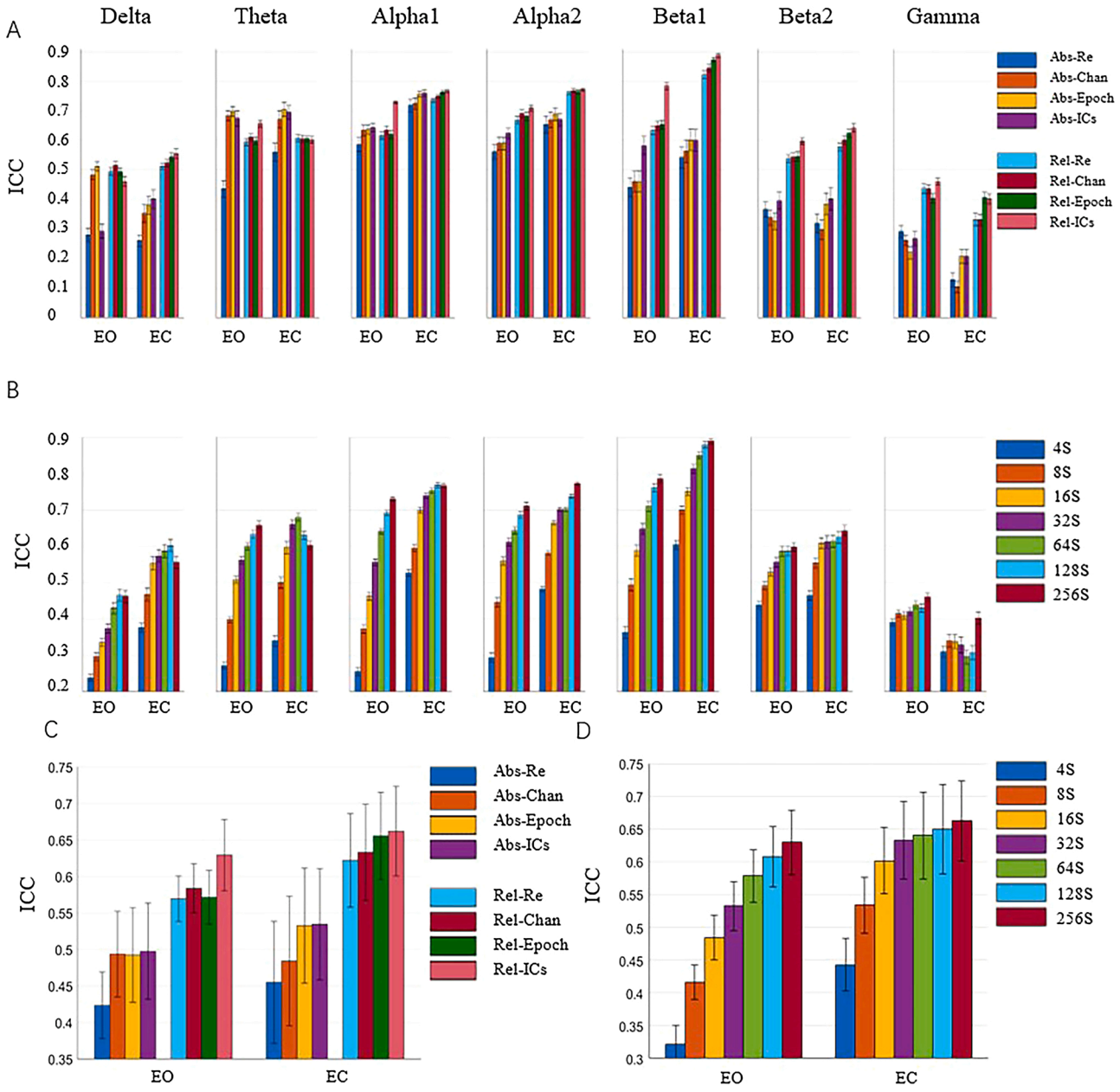

Fig. 1. The influence of pre-processing steps, data durations, resting conditions, and power types on the reproducibility of power spectrum. (A) The influence of pre-processing steps on the ICC values of absolute and relative power. (B) The influence of data durations on the ICC values of the relative power. The ICC of pre-processing steps (C) and data durations (D) after averaged among 7 frequency bands. The standard error was calculated by 63 channels for A&B, and by 7 frequency bands for C&D. EC: eyes-closed; EO: eyes-open; Abs: absolute power; Rel: relative power; Re: Re-reference; Chan: Reject channel; Epoch: Reject epoch, ICs: Reject ICs.

had the highest reproducibility in EO and EC respectively. The ICC value showed an inverted U-shaped trend from the low- to high-frequency band (Fig. 1A). Notice that the relative power was more repeatable than the absolute power in most frequency bands (except the theta band). Generally, pre-processing was important for improving the reproducibility of power. There were gradual improvements with adding steps of pre-processing. Besides, Reject ICs was strongly recommended for rsEEG of EO (Fig. 1C).

For the effect of data duration, we fixed the pre-processing to the best one with all steps and the power type to relative power. With the increase of data duration, more stable rhythm power would be obtained in low-frequency bands (beta2 and below). However, in the gamma band, increasing the data duration did not improve the reproducibility (see Fig. 1B). On average, the reproducibility of power in EO enhanced with the increase of data duration, and until 128 s that there was no significant difference compared with full-length data, $t(62) = 1.88$, $p = 0.38$ with Bonferroni correction. Meanwhile, we found that data with a duration of 32 s has reached a stable ICC around 0.65 for rsEEG of EC, $t(62) = 2.23$, $p = 0.16$ with Bonferroni correction (Fig. 1D).

In Table 1, we listed all the ICC values of each condition after averaged among 7 frequency bands. We conducted a 3-way repeated measurement ANOVA, i.e., 4 pre-processing steps (Re-reference / Reject Channel/ Reject Epoch/Reject ICs) × 2 power types (absolute and relative power) × 2 resting conditions (EO and EC). The mean effects of both pre-processing steps and power types were significant, with $F(3,18) = 8.3$, $p < 0.01$, $\eta 2\ p = 0.581$, and $F(1,6) = 10.4$, $p < 0.05$, $\eta 2\ p = 0.581$, respectively. However, the main effect of resting conditions were not significant ($F(1,6) = 2.0$, $p = 0.2$).

For data duration in Table 2, we conducted a two-way repeated measurement ANOVA (7 durations × 2 resting conditions). We found significant main effects of duration and resting condition (marginal significance) after Greenhouse-Geisser, with $F(1.213,7.277) = 27.4$, $p < 0.001$, $\eta 2\ p = 0.820$, and $F(1,6) = 5.8$, $p = 0.052$, $\eta 2\ p = 0.493$, respectively.

3.2. Topography analysis

The topography revealed that the sensors had high reproducibility in theta, alpha and beta1 bands (Fig. 2). Furthermore, the occipital area seemed to be the most stable region in the seven frequency bands, in both EC and EO conditions. Compared with absolute power, the ICC distribution of relative power was smoother. Generally, ICC has a symmetric distribution between the left and right hemispheres. As rsEEG usually had higher reproducibility in EC than in EO, hereafter, we only used the data in EC with full pre-processing steps and the full duration of 5 min for the following analysis.

3.3. Source-level power spectrum analysis

In this analysis, the ICC values of 8196 dipoles' relative power in the EC condition were calculated in each frequency band. Considering clarity, we calculated each AAL brain region's ICC values of power spectrum by averaging ICC values of the dipoles in each ROI region and all frequency bands. This resulted in a single ICC value for each AAL region (see Fig. 3). The stability of the parieto-occipital lobes was better than that of the frontal, temporal and marginal lobes. Next to the color bar was the ICC value of each AAL region. Among them, the most stable region was the posterior cingulate cortex (AAL = 39, ICC = 0.71), while the most unstable region was the orbitofrontal cortex (AAL = 27, ICC = 0.36).

Table 1
The ICC values for pre-processing steps, resting conditions and power types.

		Re-reference	Reject channels	Reject epochs	Reject ICs
Eyes-open	Absolute power	0.42	0.49	0.49	0.50
	Relative power	0.57	0.58	0.57	0.63
Eyes-closed	Absolute power	0.46	0.48	0.53	0.54
	Relative power	0.62	0.63	0.65	0.66

Table 2
The ICC values of relative power for resting conditions and data durations.

	4 s	8 s	16 s	32 s	64 s	128 s	256 s
Eyes-open	0.32	0.42	0.49	0.53	0.58	0.61	0.63
Eyes-closed	0.44	0.53	0.60	0.63	0.64	0.65	0.66

3.4. Sensor-level connectivity analysis

The ICC values of the connectivity in the sensor-level exhibited an inverted U-shaped distribution and reached the highest value in the alpha1 band (Fig. 4A). Compared with the insensitive to volume conduction connectivity measures (IMC, LGC, WPLI, PLI, and PEC), the three sensitive to volume conduction measures (PLV, COH, and RHO) had higher ICC values (Fig. 4B). More importantly, among the five insensitive to volume conduction measures, PEC had the best performance with ICC of 0.387.

By calculating the correlation between all pairs of the eight connectivity measures, we investigated the similarity of different indexes. In this analysis, ICC values of all links of each measure, i.e., $(63 \times 62)/2$, were the inputs for the correlation analysis. The correlation matrix of the eight connectivity measures could be divided into two clusters (see Fig. 4C), the three measures were highly correlated (COH, RHO, and PLV), and were considerably different from the other five measures (IMC, LGC, WPLI, PLI, and PEC). Interestingly, this classification was consistent with the definition of sensitive/insensitive to volume conduction.

In the topography diagram of the sensor-level connectivity, the edges with the highest 1 % ICC values were illustrated in Fig. 4D. Among them, the difference between sensitive and insensitive to volume conduction measures was easy to be identified.

3.5. Source-level connectivity analysis

To explore the reproducibility of different construction methods for the whole-brain network, the ICC values were averaged among all edges, and frequency bands (see Fig. 5A and Table 3). We conducted a 2-way repeated measurement ANOVA, with 4 whole-brain network constructions (AVE, PCA, CDR, and SFM) × 8 connectivity measures. The main effects of both construction strategies and connectivity measures were significant after Greenhouse-Geisser correction, with $F(1.285,7.713) = 27.29$, $p < 0.01$, $\eta 2\ p = 0.82$; and $F(1.535,9.209) = 9.72$, $p < 0.01$, $\eta 2\ p = 0.618$, respectively. Our post-hoc tests revealed two interesting results. On the one hand, SFM performed the best among these four network constructions (with $t = 15.5$, $p < 0.01$; $t = 9.5$, $p < 0.01$; and $t = 12.1$, $p < 0.01$ when SFM compared with PCA, AVG and CDR respectively, with Bonferroni correction). On the other hand, PEC showed the best performance among the five insensitive to volume conduction measures (with $t = 7.9$, $p < 0.01$; $t = 8.6$, $p < 0.01$; and $t = 7.1$, $p < 0.01$; and $t = 1.8$, $p = 1.0$ when PEC compared with WPI, IMC, LGC and PLI respectively, with Bonferroni correction).

For simplicity, we only used SFM as the whole-brain network construction, averaging all frequency bands. The edges of the highest 1 % ICC values were illustrated in Fig. 5B. Most edges were distributed around the occipital and parietal lobes, with a similar pattern to the power spectrum illustrated in Fig. 3.

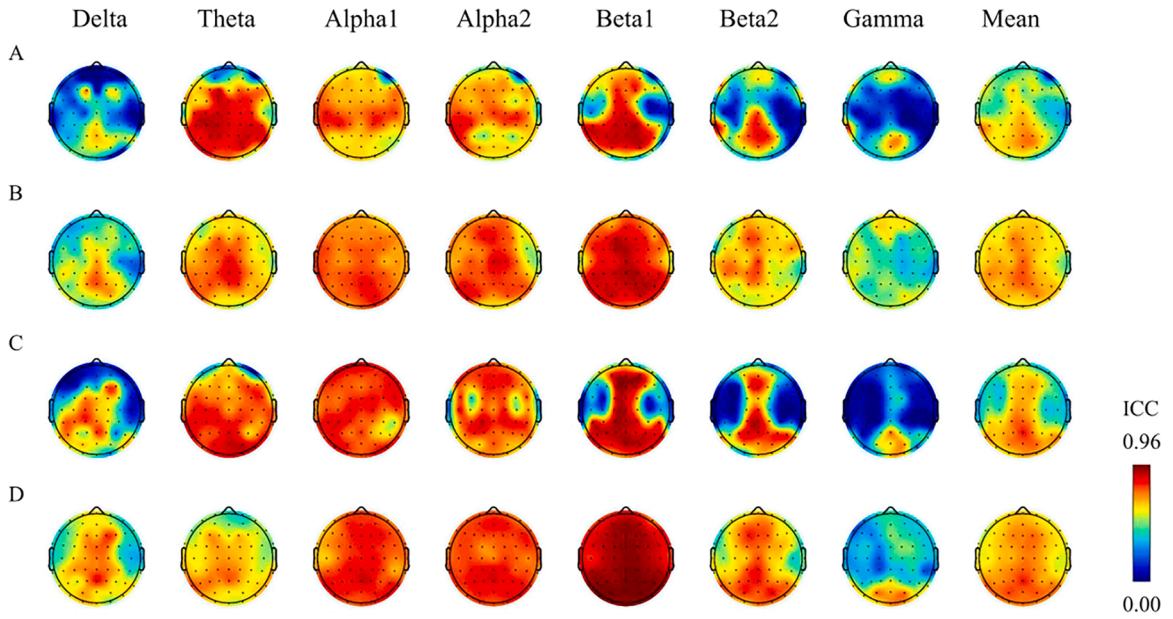

Fig. 2. The topography of ICC values in seven frequency bands and the mean of all frequency bands. The ICC values of (A) absolute power in EO, (B) relative power in EO, (C) absolute power in EC, (D) relative power in EC.

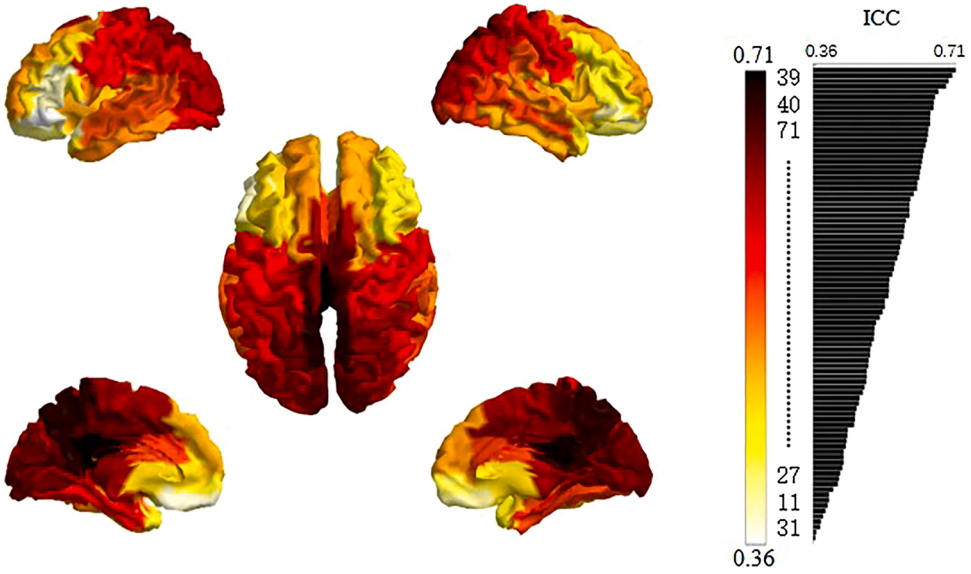

Fig. 3. The ICC value of relative power in source-level in EC, averaged across 7 frequency bands. For the ICC bar, the vertical axis corresponds to ICC value and the horizontal axis corresponds to AAL regions, sorted in descending order.

4. Discussion

The primary purpose of our study was to quantify the reproducibility of sensor- and source-level spectral powers, connectivity measures, and network constructions for resting-state EEG. We found the reproducibility of the source-level power was lower than that of the sensor-level. As summarized in Fig. 6, the sensor-level power spectrum had the highest ICC, and finally the functional connectivity in source-level. The reproducibility in eyes-closed condition was slightly higher than that in eyes-open condition, both for power and connectivity, see Supplementary Figs. S2–S4 for the result of EO. Relative power is more repeatable than the absolute power in most frequency bands (except the theta band). Remarkably, connectivity measures could be separated into two classes according to their reproducibility, and this classification is consistent with the definition of sensitive/insensitive to volume conduction. In general, the reproducibility of PEC was the highest among five insensitive to volume conduction measures. Furthermore, compared with the three common ways to construct the whole-brain network, the simplified forward model with only one center dipole within each ROI obtained the highest reproducibility. Taken together, we conducted a systematic experimental test on the reproducibility of multiple methods related to the resting-state EEG.

4.1. Power spectrum analysis

In this study, we found that the reproducibility of power spectrum of EC was slightly higher than that of EO, both in relative and absolute power. This result was in line with a previous study (Corsi-Cabrera et al., 2007). In addition to the inherent differences in EEG activity between these two conditions, another two important factors also influence the

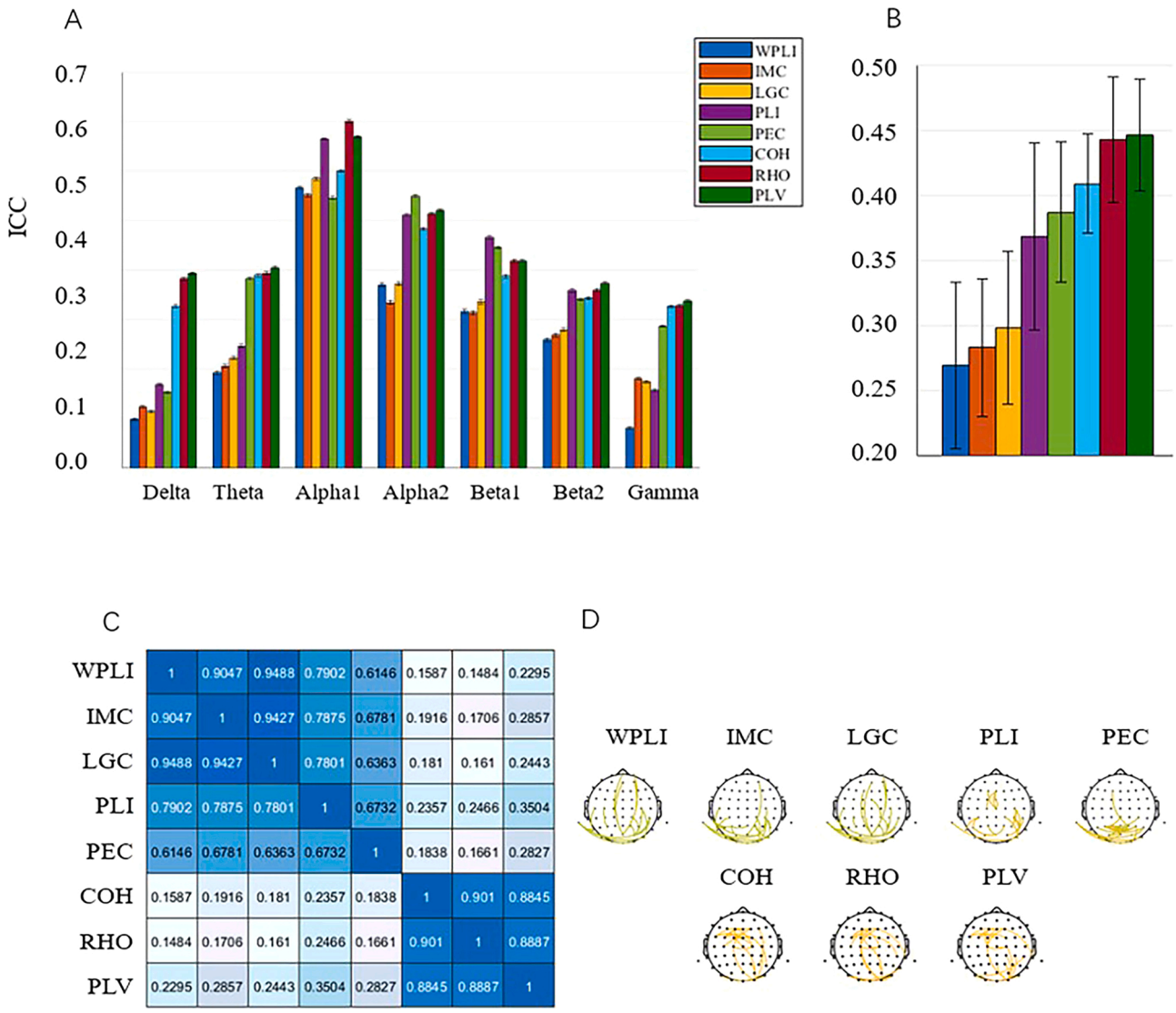

Fig. 4. ICC values of eight functional connectivity measures in sensor-level in EC. (A) ICC values of eight connectivity measures in seven frequency bands. The standard error was calculated by 63 channels. (B) The mean ICC values of the seven frequency bands. The standard error was calculated by 7 frequency bands. (C) The correlation between the ICC values of eight connectivity measures, and two clusters could be identified. (D) Topological diagram of the highest 1 % ICC values of the eight measures. See the main text for the abbreviation of connectivity measures.

reproducibility. On the one hand, the dominant electric power, especially the alpha and beta1 bands, was much larger in EC than that in EO. This may greatly increase the consistency of the signal of EC. On the other hand, these two conditions were associated with different eye movements (van Diessen et al., 2015), which also influenced the reproducibility. However, some participants would fall asleep even in short periods of resting-state measurements (Tagliazucchi and Laufs, 2014). We found that there were 18 recordings (total recordings: 171) including more than 1-minutes slight sleep (N1 sleep) epochs. We excluded these signals and recalculated the ICC of power in sensor-level using full preprocessed data, and the results were similar to the initial results.

As the signal-to-noise ratio defines how well a signal can be measured, it is a reasonable assumption that the reproducibility is strongly affected by the overall power. However, in terms of ICC calculation process, ICC values mainly depend on the variance rather than the mean values. Furthermore, we have added an analysis of the correlation between mean relative power and ICC at sensor-level. The result shows that there is no direct relationship between ICC and relative power. The correlation between them varied among different frequency bands. In theta, alpha1, and alpha2 bands, the relative power was positively correlated with the ICC of the power spectrum. On the contrary, in other frequency bands, the relative power was negatively correlated with the ICC of power spectrum. (See Supplementary Fig. S1 and Table S1 for more information).

The difference between EC and EO was observed regarding the total EEG length used for frequency analysis. When averaging ICC for all frequency bands, a 32-s recording had nearly the same reproducible as a 256 s recording in EC. This was in accord with two previous studies that claimed the validity of short recording (Möcks and Gasser, 1984; Salinsky et al., 1991). However, in EO condition, with the increase of data duration, the reproducibility also enhanced substantially. This indicates that for frequency analysis, it is better to collect data for a longer duration for more than 2 min in EO conditions, while half a minute of data may be acceptable in EC.

Generally, our data showed that the relative power was more reproducible than absolute power. In theta and alpha bands, relative power and absolute power exhibited similar reproducibility, and this was consistent with many previous studies (Fein et al., 1983; Gasser et al., 1985; Salinsky et al., 1991). Nonetheless, higher ICC values were

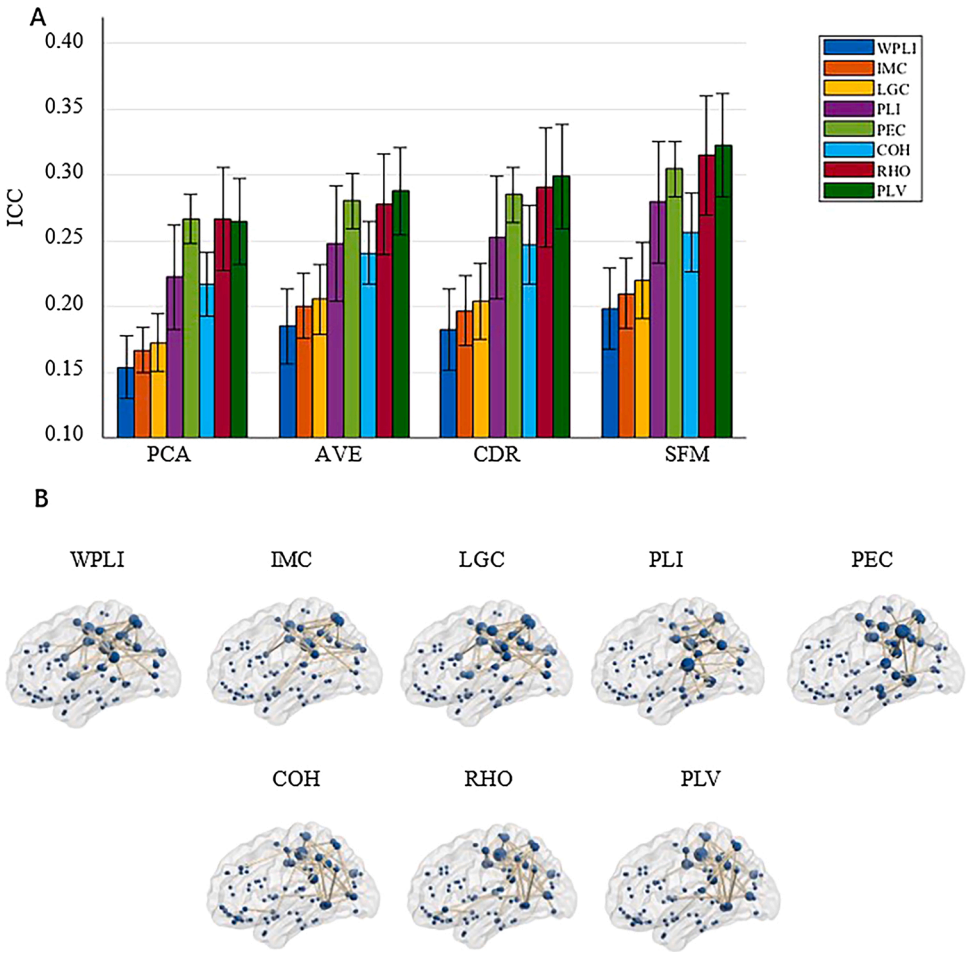

Fig. 5. (A) The ICC values of four network construction methods averaged among the seven frequency bands in EC. The standard error was calculated by 7 frequency bands. (B) the edges of the highest 1 % ICC values with SFM and averaged among all frequency bands. The size of the node represents the number of its adjacent edge. PCA: The first principal component within each ROI; AVE: The average within each ROI; CDR: The center dipole representative; SFM: The simplified forward model; See the main text for the abbreviation of connectivity measures.

Table 3
The ICC values of connectivity measures and whole-brain network constructions.

	WPLI	IMC	LGC	PLI	PEC	COH	RHO	PLV
PCA	0.15	0.17	0.17	0.22	0.27	0.22	0.27	0.26
AVE	0.19	0.20	0.21	0.25	0.28	0.24	0.28	0.29
CDR	0.18	0.20	0.20	0.25	0.29	0.25	0.29	0.30
SFM	0.20	0.21	0.22	0.28	0.30	0.26	0.31	0.32

Notes: PCA: The first principal component within each ROI; AVE: The average within each ROI; CDR: The center dipole representative; SFM: The simplified forward model; See the main text for the abbreviation of connectivity measures.

found for relative power in beta and gamma bands. A possible interpretation is that the relative power becomes reproducible because of the stable and unique power spectral pattern for each person (Napflin et al., 2007), and the normalizing step greatly emphasized the spectral pattern. Moreover, as shown in Fig. 2, for relative power, the distribution is smoother in high-frequency bands, leading to a higher ICC of the whole scalp. But for absolute power, in the delta, beta2, and gamma bands, the reproducibility of frontal and temporal areas were poor, which might be due to the interference of eye movement and muscle artifacts (Hipp and Siegel, 2013; Yuval-Greenberg et al., 2008) or the loose link between skin and electrode.

4.2. Sensor or source-level

Consistent with a previous study (Moezzi et al., 2018), we found the reproducibility of source-level measures was lower than that of the sensor-level one, both in power and connectivity.

For the frequency analysis, we found that the occipital area was the most reproducible region for both EC and EO conditions. Meanwhile, in the source-level, the reproducibility of the parieto-occipital lobe was better than that of the frontal and temporal lobes, like a source space projection of sensor topology of ICC. There was a similar projection for the ICC of functional connectivity. The performance ranking of each connectivity measures at the source-level was consistent with that in the sensor-level. Moreover, no connectivity measure performed better at the source-level than at the sensor-level. As we know, EEG source space analysis could be helpful in demixing and purifying signals (Michel and Murray, 2012). More importantly, source space analysis corresponded with the structural anatomy of the brain in detail and had great potential in clinical and experimental applications. So, in our view, even though it has a higher reproducibility in the sensor-level, analysis in the source space was of great worth.

4.3. Connectivity measures

Consistent with the MEG study (Colclough et al., 2016), we found that compared with five insensitive to volume conduction measures (IMC, LGC, WPLI, PLI, and PEC), those sensitive to volume conduction measures (PLV, COH, and RHO) had higher ICC values both in sensor- and source-level. This high ICC value may be due to their shortcomings (sensitive to volume conduction), i.e., they generate lots of consistent, strong, spurious connections over repeated sessions and these spurious connections have good discrimination in different participants, thus leading to a high ICC value. So we did not recommend the use of these sensitive to volume conduction connectivity measures.

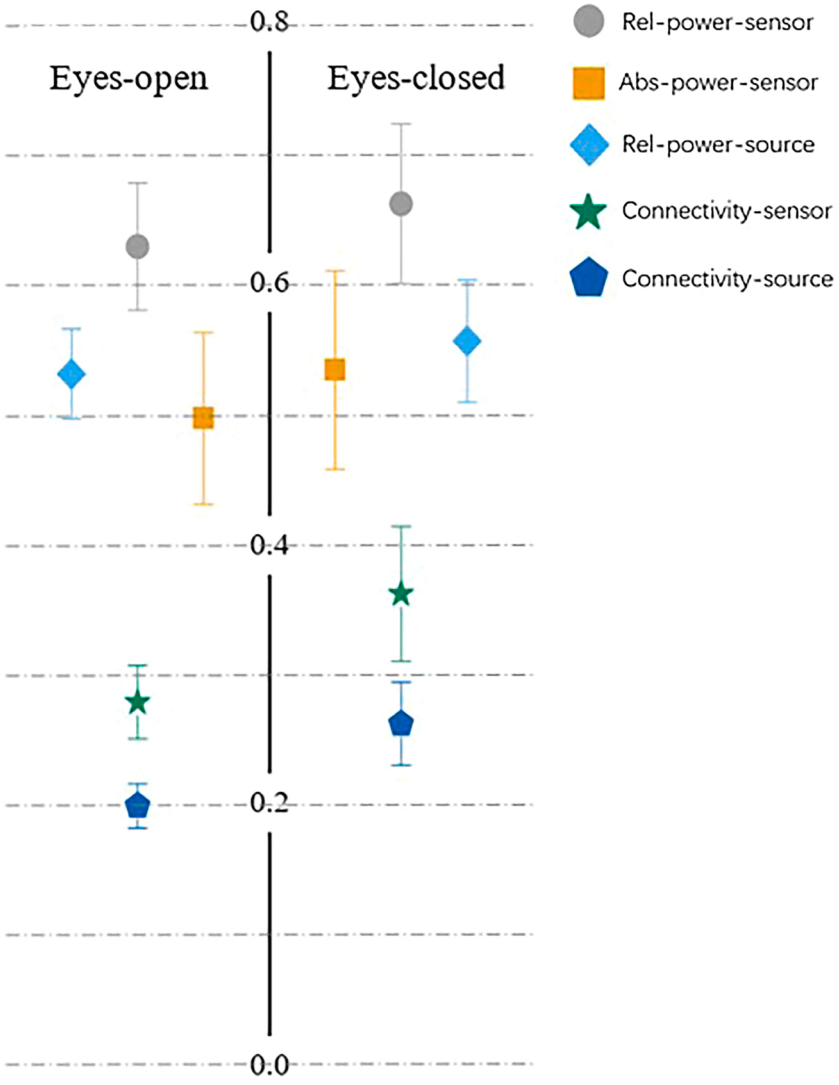

Fig. 6. The ICC values of power and connectivity. The ICC of the power is the average of all electrodes/dipoles and all frequency bands, and the ICC of the connectivity is the average of all connection edges, all connectivity measures and frequency bands. The standard error was calculated by seven frequency bands. Rel-power-sensor: ICC of Relative power in sensor level; Abs-power-sensor: ICC of absolute power in sensor level; Rel-power-source: ICC of Relative power in source level; Connectivity-sensor: ICC of connectivity in sensor level; Connectivity-source: ICC of connectivity in source level.

Nolte and colleagues found that some connectivity measures turned out to be the functions of lagged coherence for data with Gaussian distributed (Nolte et al., 2019). Our research was to explore the correlation between the connectivity measures from the perspective of reproducibility. We found that functional connectivity measures could be separated into two classes, and each had a similar reproducibility in connectivity estimation (Fig. 4C). One class contains those sensitive to volume conduction measures which are sensitive to volume conduction (PLV, COH, and RHO); another one was insensitive to volume conduction (IMC, LGC, WPLI, PLI, and PEC). This showed that the stability of different measures was highly similar within a class. Of different measures, their overall ICC values could be distinct from each other but had little impact on the order of edge's ICC. That is to say, an edge's ranking of stability depended on itself, rather than the selection of connectivity methods (see Figs. 4D and 5 B).

Notably, among the 5 measures insensitive to volume conduction, the reproducibility of PEC was the highest, for both the sensor and source-level, and this is consistent with a previous MEG study (Colclough et al., 2016).

The reproducibility of PLI was the highest among those phase-based insensitive to volume conduction measures. According to recent studies (Daffertshofer et al., 2018; Siems and Siegel, 2020), phase-based and amplitude-based measures of connectivity might have inherently different features. Therefore, from the point of reproducibility, PEC and PLI were recommended separately here for each type of connectivity measure of rsEEG.

4.4. Network construction

To our knowledge, our current study was the first to investigate the influence of signal extraction in the network construction of rsEEG. The previous study of network construction focused on the weighted network or unweighted network, directed or undirected network, or the selection of ROI template. Extracting signal from an ROI was rarely discussed but was very important for rsEEG. For fMRI, taking the mean or extract the first Eigen variate (as done in SPM, http://www.fil.ion.ucl.ac.uk/spm) of a region was straightforward. Though the simplified forward model we proposed here had the best reproducibility, we found that the connectivity values calculated by four network construction strategies were highly correlated ($r = 0.85$). Compared with the results of Mahjoory et al. (2017), this correlation is higher than that of different inverse methods and analysis toolboxes ($r = 0.61$ and $r = 0.70$, respectively), and lower than that of different forward models ($r = 0.97$). More importantly, simplify the forward model greatly reduced the amount of calculation. However, the drawback of this method is that the geometric properties of each ROI were ignored, and future researches are needed to reveal more features of this method.

4.5. Limitation

For data analysis of rsEEG, there are many possible pipelines. Here we restricted our investigation on some critical approaches in practice, while fixed other parameters. However, this constituted an obvious drawback of our current study. First, in EEG power analysis, we took the traditional approach but not using those new methods such as 'setting the rhythm's range with their oscillatory peaks' or 'removing the 1/f-component from the power spectrum' (Haller et al., 2018). Second, we only chose the undirected connectivity measures, without considering directed connectivity nor the partial correlation. Third, it may be argued that other ROIs templates would have been more representative of state-of-the-art studies. Fourth, we fixed the dipoles with vertical direction of cortex surface, rather than using free direction. The source-level connectivity analysis with free direction is more complicated, and this issue will be discussed in detail in our future study. Moreover, this study only focused on the resting-state EEG, and caution is necessary when extending our results to event-related potentials or EEG of natural stimuli, such as movie watching and music listening. Last but not least, only one source reconstruction pipeline was used in the current study. There were many other source imaging pipelines. Although their reproducibility has been well discussed in a previous study (Mahjoory et al., 2017), their interaction with connectivity measures and network construction needs further investigation.

5. Conclusion

Our current study showed that the reproducibility of rsEEG during eyes-closed condition was slightly higher than that of eyes-open condition. Besides, the reproducibility of relative power was higher than that of absolute power. On average, a comprehensive preprocess with full steps and longer data duration for more than 5 min could improve the reproducibility, especially for EO. Remarkably, connectivity measures could be separated into two classes according to their ICC values. Meanwhile, among the five insensitive to volume conduction measures, the reproducibility of PEC was the highest. Finally, the simplified forward model obtained the higher reproducibility among the four ways to construct whole-brain network. Taken together, our results described the reproducibility of rsEEG power spectrum, connectivity measures, and network constructions, which could be considered in assessing inter-individual differences in brain-behavior relationships, as well as in automatic biometric applications.

CRediT authorship contribution statement

Wei Duan: Conceptualization, Investigation, Software, Formal analysis, Writing - original draft. **Xinyuan Chen:** Formal analysis, Writing - review & editing. **Ya-Jie Wang:** Writing - review & editing. **Wenrui Zhao:** Formal analysis. **Hong Yuan:** Resources. **Xu Lei:** Conceptualization, Writing - review & editing, Supervision, Project administration, Funding acquisition.

Declaration of Competing Interest

The authors report no declarations of interest.

Acknowledgments

This work was supported by the National Natural Science Foundation of China (grant number 31971028) and Major Project of Medicine Science and Technology of PLA (AWS17J012).

Appendix A. Supplementary data

Supplementary material related to this article can be found, in the online version, at doi:https://doi.org/10.1016/j.jneumeth.2020.108985.

References

Agcaoglu, O., Wilson, T.W., Wang, Y.P., Stephen, J., Calhoun, V.D., 2019. Resting state connectivity differences in eyes open versus eyes closed conditions. Hum. Brain Mapp. 40 (8), 2488–2498. https://doi.org/10.1002/hbm.24539.

Babiloni, C., Lizio, R., Percio, C., Marzano, N., Soricelli, A., Salvatore, E., et al., 2013. Cortical sources of resting state EEG rhythms are sensitive to the progression of early stage Alzheimer's disease. J. Alzheimers Dis. 34. https://doi.org/10.3233/JAD-121750.

Bruder, G.E., Sedoruk, J.P., Stewart, J.W., McGrath, P.J., Quitkin, F.M., Tenke, C.E., 2008. Electroencephalographic alpha measures predict therapeutic response to a selective serotonin reuptake inhibitor antidepressant: pre- and post-treatment findings. Biol. Psychiatry 63 (12), 1171–1177. https://doi.org/10.1016/j.biopsych.2007.10.009.

Colclough, G.L., Woolrich, M.W., Tewarie, P.K., Brookes, M.J., Quinn, A.J., Smith, S.M., 2016. How reliable are MEG resting-state connectivity metrics? Neuroimage 138, 284–293. https://doi.org/10.1016/j.neuroimage.2016.05.070.

Corsi-Cabrera, M., Galindo-Vilchis, L., del-Rio-Portilla, Y., Arce, C., Ramos-Loyo, J., 2007. Within-subject reliability and inter-session stability of EEG power and coherent activity in women evaluated monthly over nine months. Clin. Neurophysiol. 118 (1), 9–21. https://doi.org/10.1016/j.clinph.2006.08.013.

Daffertshofer, A., Ton, R., Kringelbach, M.L., Woolrich, M., Deco, G., 2018. Distinct criticality of phase and amplitude dynamics in the resting brain. Neuroimage 180 (Pt B), 442–447. https://doi.org/10.1016/j.neuroimage.2018.03.002.

Deco, G., Jirsa, V.K., McIntosh, A.R., 2011. Emerging concepts for the dynamical organization of resting-state activity in the brain. Nat. Rev. Neurosci. 12 (1), 43–56. https://doi.org/10.1038/nrn2961.

Deuker, L., Bullmore, E.T., Smith, M., Christensen, S., Nathan, P.J., Rockstroh, B., Bassett, D.S., 2009. Reproducibility of graph metrics of human brain functional networks. Neuroimage 47 (4), 1460–1468. https://doi.org/10.1016/j.neuroimage.2009.05.035.

Fein, G., Galin, D., Johnstone, J., Yingling, C.D., Marcus, M., Kiersch, M.E., 1983. EEG power spectra in normal and dyslexic children. I. Reliability during passive conditions. Electroencephalogr. Clin. Neurophysiol. 55 (4), 399–405. https://doi.org/10.1016/0013-4694(83)90127-x.

Gasser, T., Bächer, P., Steinberg, H., 1985. Test-retest reliability of spectral parameters of the EEG. Electroencephalogr. Clin. Neurophysiol. 60 (4), 312–319. https://doi.org/10.1016/0013-4694(85)90005-7.

Greicius, M.D., Krasnow, B., Reiss, A.L., Menon, V., 2003. Functional connectivity in the resting brain: a network analysis of the default mode hypothesis. Proc. Natl. Acad. Sci. U. S. A. 100 (1), 253–258. https://doi.org/10.1073/pnas.0135058100.

Haller, M., Donoghue, T., Peterson, E., Varma, P., Sebastian, P., Gao, R., et al., 2018. Parameterizing Neural Power Spectra. bioRxiv, p. 299859. https://doi.org/10.1101/299859.

Hipp, J., Siegel, M., 2013. Dissociating neuronal gamma-band activity from cranial and ocular muscle activity in EEG. Front. Hum. Neurosci. 7, 338. https://doi.org/10.3389/fnhum.2013.00338.

Hipp, J.F., Hawellek, D.J., Corbetta, M., Siegel, M., Engel, A.K., 2012. Large-scale cortical correlation structure of spontaneous oscillatory activity. Nat. Neurosci. 15 (6), 884–890. https://doi.org/10.1038/nn.3101.

Holmes, C.J., Hoge, R., Collins, L., Woods, R., Toga, A.W., Evans, A.C., 1998. Enhancement of MR images using registration for signal averaging. J. Comput. Assist. Tomogr. 22 (2), 324–333. https://doi.org/10.1097/00004728-199803000-00032.

Iandolo, R., Chiappalone, M., Semprini, M., Buccelli, S., Barban, F., Zhao, M., et al., 2020. Small-world propensity reveals the frequency specificity of resting state networks. IEEE Open Journal of Engineering in Medicine and Biology. https://doi.org/10.1109/OJEMB.2020.2965323, 1-1.

Koenig, T., Studer, D., Hubl, D., Melie, L., Strik, W.K., 2005. Brain connectivity at different time-scales measured with EEG. Philos Trans. R. Soc. Lond. B Biol. Sci. 360 (1457), 1015–1023. https://doi.org/10.1098/rstb.2005.1649.

Lachaux, J.P., Rodriguez, E., Martinerie, J., Varela, F.J., 1999. Measuring phase synchrony in brain signals. Hum. Brain Mapp. 8 (4), 194–208. https://doi.org/10.1002/(sici)1097-0193(1999)8:4<194::aid-hbm4>3.0.co;2-c.

Mahjoory, K., Nikulin, V.V., Botrel, L., Linkenkaer-Hansen, K., Fato, M.M., Haufe, S., 2017. Consistency of EEG source localization and connectivity estimates. Neuroimage 152, 590–601. https://doi.org/10.1016/j.neuroimage.2017.02.076.

Martín-Buro, M.C., Garcés, P., Maestú, F., 2016. Test-retest reliability of resting-state magnetoencephalography power in sensor and source space. Hum. Brain Mapp. 37 (1), 179–190. https://doi.org/10.1002/hbm.23027.

Michel, C.M., Murray, M.M., 2012. Towards the utilization of EEG as a brain imaging tool. Neuroimage 61 (2), 371–385. https://doi.org/10.1016/j.neuroimage.2011.12.039.

Möcks, J., Gasser, T., 1984. How to select epochs of the EEG at rest for quantitative analysis. Electroencephalogr. Clin. Neurophysiol. 58 (1), 89–92. https://doi.org/10.1016/0013-4694(84)90205-0.

Moezzi, B., Hordacre, B., Berryman, C., Ridding, M.C., Goldsworthy, M.R., 2018. Test-retest Reliability of Functional Brain Network Characteristics Using Resting-state EEG and Graph Theory. bioRxiv, p. 385302. https://doi.org/10.1101/385302.

Mosher, J., Leahy, R., Lewis, P., 1999. EEG and MEG: forward solutions for inverse methods. IEEE Trans. Biomed. Eng. 46, 245–259. https://doi.org/10.1109/10.748978.

Muthukumaraswamy, S.D., 2013. High-frequency brain activity and muscle artifacts in MEG/EEG: a review and recommendations. Front. Hum. Neurosci. 7, 138. https://doi.org/10.3389/fnhum.2013.00138.

Napflin, M., Wildi, M., Sarnthein, J., 2007. Test-retest reliability of resting EEG spectra validates a statistical signature of persons. Clin. Neurophysiol. 118 (11), 2519–2524. https://doi.org/10.1016/j.clinph.2007.07.022.

Nolte, G., Bai, O., Wheaton, L., Mari, Z., Vorbach, S., Hallett, M., 2004. Identifying true brain interaction from EEG data using the imaginary part of coherency. Clin. Neurophysiol. 115 (10), 2292–2307. https://doi.org/10.1016/j.clinph.2004.04.029.

Nolte, G., Galindo-Leon, E., Li, Z., Liu, X., Engel, A.K., 2019. Mathematical Relations Between Measures of Brain Connectivity Estimated From Electrophysiological Recordings for Gaussian Distributed Data. bioRxiv, p. 680678. https://doi.org/10.1101/680678.

Nunez, P.L., Srinivasan, R., Westdorp, A.F., Wijesinghe, R.S., Tucker, D.M., Silberstein, R. B., Cadusch, P.J., 1997. EEG coherency. I: statistics, reference electrode, volume conduction, Laplacians, cortical imaging, and interpretation at multiple scales. Electroencephalogr. Clin. Neurophysiol. 103 (5), 499–515. https://doi.org/10.1016/s0013-4694(97)00066-7.

Pascual-Marqui, R., Lehmann, D., Koukkou, M., Kochi, K., Anderer, P., Saletu, B., et al., 2011. Assessing interactions in the brain with exact low resolution electromagnetic tomography (eLORETA). Philos. Trans. Series A Math. Phys. Eng. Sci. 369, 3768–3784. https://doi.org/10.1098/rsta.2011.0081.

Pion-Tonachini, L., Kreutz-Delgado, K., Makeig, S., 2019. ICLabel: an automated electroencephalographic independent component classifier, dataset, and website. Neuroimage 198, 181–197. https://doi.org/10.1016/j.neuroimage.2019.05.026.

Rolls, E.T., Huang, C.C., Lin, C.P., Feng, J., Joliot, M., 2020. Automated anatomical labelling atlas 3. Neuroimage 206, 116189. https://doi.org/10.1016/j.neuroimage.2019.116189.

Rotondi, F., Franceschetti, S., Avanzini, G., Panzica, F., 2016. Altered EEG resting-state effective connectivity in drug-naïve childhood absence epilepsy. Clin. Neurophysiol. 127 (2), 1130–1137. https://doi.org/10.1016/j.clinph.2015.09.003.

Salinsky, M.C., Oken, B.S., Morehead, L., 1991. Test-retest reliability in EEG frequency analysis. Electroencephalogr. Clin. Neurophysiol. 79 (5), 382–392. https://doi.org/10.1016/0013-4694(91)90203-g.

Schoffelen, J.-M., Gross, J., 2009. Source connectivity analysis with MEG and EEG. Hum. Brain Mapp. 30, 1857–1865. https://doi.org/10.1002/hbm.20745.

Shrout, P.E., Fleiss, J.L., 1979. Intraclass correlations: uses in assessing rater reliability. Psychol. Bull. 86 (2), 420–428. https://doi.org/10.1037//0033-2909.86.2.420.

Siebenhuhner, F., Weiss, S.A., Coppola, R., Weinberger, D.R., Bassett, D.S., 2013. Intra- and inter-frequency brain network structure in health and schizophrenia. PLoS One 8 (8), e72351. https://doi.org/10.1371/journal.pone.0072351.

Siems, M., Siegel, M., 2020. Dissociated neuronal phase- and amplitude-coupling patterns in the human brain. Neuroimage 209, 116538. https://doi.org/10.1016/j.neuroimage.2020.116538.

Smit, D.J., Posthuma, D., Boomsma, D.I., Geus, E.J., 2005. Heritability of background EEG across the power spectrum. Psychophysiology 42 (6), 691–697. https://doi.org/10.1111/j.1469-8986.2005.00352.x.

Stam, C.J., Nolte, G., Daffertshofer, A., 2007. Phase lag index: assessment of functional connectivity from multi channel EEG and MEG with diminished bias from common sources. Hum. Brain Mapp. 28 (11), 1178–1193. https://doi.org/10.1002/hbm.20346.

Tagliazucchi, E., Laufs, H., 2014. Decoding wakefulness levels from typical fMRI resting-state data reveals reliable drifts between wakefulness and sleep. Neuron 82, 695–708. https://doi.org/10.1016/j.neuron.2014.03.020.

Tass, P., Rosenblum, M., Weule, J., Kurths, J., Pikovsky, A., Volkmann, J., et al., 1998. Detection of n:m phase locking from noisy data: application to magnetoencephalography. Phys. Rev. Lett. 81, 3291–3294. https://doi.org/10.1103/PhysRevLett.81.3291.

Tomescu, M.I., Rihs, T.A., Rochas, V., Hardmeier, M., Britz, J., Allali, G., et al., 2018. From swing to cane: sex differences of EEG resting-state temporal patterns during maturation and aging. Dev. Cogn. Neurosci. 31, 58–66. https://doi.org/10.1016/j.dcn.2018.04.011.

van Diessen, E., Numan, T., van Dellen, E., van der Kooi, A.W., Boersma, M., Hofman, D., et al., 2015. Opportunities and methodological challenges in EEG and MEG resting state functional brain network research. Clin. Neurophysiol. 126 (8), 1468–1481. https://doi.org/10.1016/j.clinph.2014.11.018.

Vinck, M., Oostenveld, R., van Wingerden, M., Battaglia, F., Pennartz, C.M.A., 2011. An improved index of phase-synchronization for electrophysiological data in the presence of volume-conduction, noise and sample-size bias. Neuroimage 55 (4), 1548–1565. https://doi.org/10.1016/j.neuroimage.2011.01.055.

Volf, N.V., Belousova, L.V., Knyazev, G.G., Kulikov, A.V., 2014. Genger differences in association between serotonin transporter gene polymorphism and resting-state EEG activity. Int. J. Psychophysiol. 94 (2), 184–185. https://doi.org/10.1016/j.ijpsycho.2014.08.777.

Yuval-Greenberg, S., Tomer, O., Keren, A., Nelken, I., Deouell, L., 2008. Transient Induced Gamma-Band Response in EEG as a Manifestation of Miniature Saccades. Neuron 58, 429–441. https://doi.org/10.1016/j.neuron.2008.03.027.